Article

Electronic Structure of Linear Thiophenolate-Bridged Heteronuclear Complexes [LFeMFeL] (M = Cr, Co, Fe; *n* = 1–3): A Combination of Kinetic Exchange Interaction and Electron Delocalization

Liviu F. Chibotaru, Jean-Jacques Girerd, Genevive Blondin, Thorsten Glaser, and Karl Wieghardt

J. Am. Chem. Soc., **2003**, 125 (41), 12615-12630• DOI: 10.1021/ja030027t • Publication Date (Web): 20 September 2003

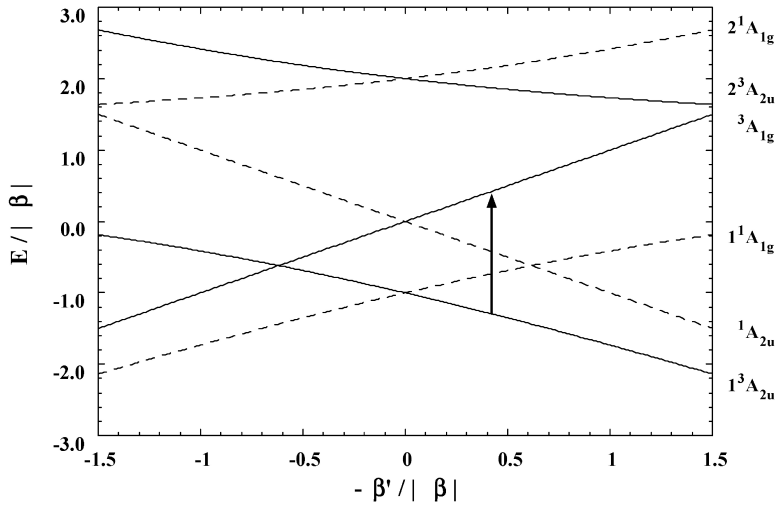

More About This Article

Additional resources and features associated with this article are available within the HTML version:

- Supporting Information
- Links to the 3 articles that cite this article, as of the time of this article download
- Access to high resolution figures
- Links to articles and content related to this article
- Copyright permission to reproduce figures and/or text from this article

View the Full Text HTML

J|A|C|S
ARTICLES
Published on Web 09/20/2003

Electronic Structure of Linear Thiophenolate-Bridged Heteronuclear Complexes $[LFeMFeL]^{n+}$ (M = Cr, Co, Fe; n = 1−3): A Combination of Kinetic Exchange Interaction and Electron Delocalization

Liviu F. Chibotaru,*,† Jean-Jacques Girerd,‡ Geneviève Blondin,‡ Thorsten Glaser,§ and Karl Wieghardt||

Contribution from the Laboratory of Quantum Chemistry, Katholieke Universiteit Leuven, Celestijnenlaan 200F, B-3001 Belgium, Laboratoire de Chimie Inorganique, URA CNRS 420, Institut de Chimie Moléculaire d'Orsay, Université Paris-Sud, 91405 Orsay, France, Institut für Anorganische und Analytische Chemie, Westfälische Wilhelms-Universität Münster, Wilhelm-Klemm-Str. 8, D-48149 Münster, Germany, and Max-Plank-Institut für Strahlenchemie, Stifstrasse 34−36, D-45470 Mülheim an der Ruhr, Germany

Received January 13, 2003; E-mail: Liviu.Chibotaru@chem.kuleuven.ac.be

Abstract: The electronic properties of the isostructural series of heterotrinuclear thiophenolate-bridged complexes of the general formula $[LFeMFeL]^{n+}$ with M = Cr, Co and Fe where L represents the trianionic form of the ligand 1,4,7-tris(4-*tert*butyl-2-mercaptobenzyl)-1,4,7-triazacyclononane, synthesized and investigated by a number of experimental techniques in the previous work[1], are subjected now to a theoretical analysis. The low-lying electronic excitations in these compounds are described within a minimal model supported by experiment and quantum chemistry calculations. It was found indeed that various experimental data concerning the magnetism and electron delocalization in the lowest states of all seven compounds are completely reproduced within a model which includes the electron transfer between magnetic orbitals at different metal centers and the electron repulsion in these orbitals (the Hubbard model). Moreover, due to the trigonal symmetry of the complexes, only the electron transfer between nondegenerate orbital, a_1, originating from the t_{2g} shell of each metal ion in a pseudo-octahedral coordination, is relevant for the lowest states. An essential feature resulting from quantum chemistry calculations, allowing to explain the unusual magnetic properties of these compounds, is the surprisingly large value and, especially, the negative sign of the electron transfer between terminal iron ions, β'. According to their electronic properties the series of complexes can be divided as follows: (1) The complexes $[LFeFeFeL]^{3+}$ and $[LFeCrFeL]^{3+}$ show localized valences in the ground electronic configuration. The strong antiferromagnetic exchange interaction and the resulting spin 1/2 of the ground-state arise from large values of the transfer parameters. (2) In the complex $[LFeCrFeL]^{+}$, due to a higher energy of the magnetic orbital on the central Cr ion than on the terminal Fe ones, the spin 3/2 and the single unpaired a_1 electron are almost localized at the chromium center in the ground state. (3) The complex $[LFeCoFeL]^{3+}$ has one ground electronic configuration in which two unpaired electrons are localized at terminal iron ions. The ground-state spin $S = 1$ arises from a kinetic mechanism involving the electron transfer between terminal iron ions as one of the steps. Such a mechanism, leading to a strong ferromagnetic interaction between distant spins, apparently has not been discussed before. (4) The complex $[LFeFeFeL]^{2+}$ is characterized by both spin and charge degrees of freedom in the ground manifold. The stabilization of the total spin zero or one of the itinerant electrons depends on β', i.e., corresponds to the observed $S = 1$ for its negative sign. This behavior does not fit into the double exchange model. (5) In $[LFeCrFeL]^{2+}$ the delocalization of two itinerant holes in a_1 orbitals takes place over the magnetic core of chromium ion. Although the origin of the ground-state spin $S = 2$ is the spin dependent delocalization, the spectrum of the low-lying electronic states is again not of a double exchange type. (6) Finally, the complex $[LFeCoFeL]^{2+}$ has the ground configuration corresponding to the electron delocalization between terminal iron atoms. The estimated magnitude of the corresponding electron transfer is smaller than the relaxation energy of the nuclear distortions induced by the electron localization at one of the centers, leading to vibronic valence trapping observed in this compound.

Introduction

The structure and the electronic properties of iron−sulfur metalloproteins and clusters are well investigated.[2−5] In these compounds, the iron ions are tetrahedrally coordinated and are found in the high-spin d^5 and d^6 electronic configurations. A remarkable feature of the iron−sulfur clusters is that several of their oxidation states are easily accessible leading to various valence distributions among iron ions. Thus, the iron atoms in the cluster can have the same valency or be of mixed valence

type. These two situations lead to different magnetic behavior. In the first case (e.g., $[Fe_2S_2]^{2+}$, $[Fe_3S_4]^{+}$) the low-lying electronic states responsible for magnetism result from the exchange interaction between total spins of the localized unpaired electrons on iron ions and are described by the conventional Heisenberg−Dirac−Van Vleck Hamiltonian.[6] In the second case (e.g., $[Fe_2S_2]^{1+}$, $[Fe_3S_4]^{0}$, $[Fe_4S_4]^{+,2+,3+}$) valence interchange between iron ions requires small promotion energy (or even zero for strictly equivalent pairs of iron sites) which means that the low-lying states will be affected by the transfer of the "excess" electrons or holes. The adequate theory of this phenomenon, called double exchange, was first developed for magnetic crystals[7−9] and later applied for the description of the magnetic properties of the mixed valence compounds.[10−15] It was found, however, that the interactions involved in the double exchange model are often not sufficient and the inclusion of the vibronic interactions[16−18] can lead to the localization of the excess particles with crucial consequences for the low-lying states and the magnetism of mixed valence compounds.[14,19,20] Although in the case of dimers this localization is complete, an intermediate situation takes place in trinuclear[21,22] and tetranuclear[23−26] iron−sulfur clusters, corresponding to a partial delocalization of the excess electrons or holes over pairs of iron atoms in these clusters.

The vibronic interaction in mixed valence clusters arise from the relaxation of the ligand environment of the metal centers as response to the change of their valences. The strength of this interaction is reflected in the difference of the average metal−ligand bond length in two valent states of the metal center. This change is known to be larger for tetrahedrally coordinated iron complexes than for octahedrally coordinated low-spin Fe^{II} and Fe^{III}. Therefore, the vibronic effects are expected to be less important and, consequently, the electron/hole delocalization more pronounced in clusters containing octahedrally coordinated iron sites.

Chart 1

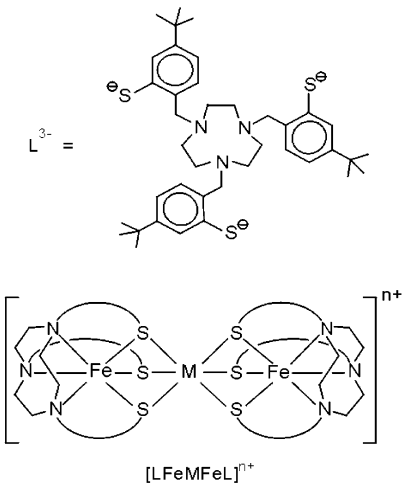

$[LFeMFeL]^{n+}$	n=1, S_t	n=2, S_t	n=3, S_t
Cr	**1a**, 3/2	**1b**, 4/2	**1c**, 1/2
Co		**2b**, 1/2	**2c**, 2/2
Fe		**3b**, 2/2	**3c**, 1/2

In the previous paper,[1] an isostructural series of heterotrinuclear thiophenolate-bridged complexes of the general formula $[LFeMFeL]^{+,2+,3+}$ with M = Fe, Co, Cr, and L, representing the trianionic form of 1,4,7-tris(4-*tert*-butyl-2-mercaptobenzyl)-1,4,7-triazacyclononane, was investigated (Chart 1). In this series, $[LFeMFeL]^{n+}$ species contain a linear array of two terminal iron ions and a central MS_6 unit, whereas the structure of the $[N_3FeS_3MS_3FeN_3]^{n+}$ core is face-sharing octahedral with six μ_2-thiolato bridges. The electronic structure of these sulfur-bridged trinuclear complexes has been investigated by a number of conventional techniques such as temperature- and field-dependent magnetochemistry, multifrequency band EPR, UV−vis/near-IR/IR, EXAFS, and XANES spectroscopies. The presence of iron atoms in the complexes allowed for additional investigation of fine details of the elctronic structure by temperature- and field-dependent Mössbauer spectroscopy. As a result, the total spin (Chart 1) as well as local spins and valences on Fe and M sites in the ground state and their changes with temperature have been firmly established for all seven compounds. Despite the common structure, these complexes show a wide range of magnetic and electronic properties. Varying M and *n* one obtains: one single spin localized on the central metal site (**1a**); two spins localized on terminal iron sites coupled ferromagnetically (**2c**); three spins localized on different metal centers coupled antiferromagnetically (**1c** and **3c**); vibronic valence trapping at low temperatures and partial delocalization of an excess electron over terminal iron sites at room temper-

† Department of Chemistry, Katholieke Universiteit Leuven.
‡ Laboratoire de Chimie Inorganique, Institut de Chimie Moléculaire d'Orsay, Université de Paris-Sud.
§ Institut für Anorganische und Analytische Chemie, Westfälische Wilhelms-Universität Münster.
|| Max-Plank-Institut für Strahlenchemie, Mülheim an der Ruhr.

(1) Glaser, T.; Beissel, T.; Bill, E.; Weyhermüller, T.; Schünemann, V.; Meyer-Klaucke, W.; Trautwein, A. X.; Wieghardt, K. *J. Am. Chem. Soc.* **1999**, *121*, 2193−2208.
(2) *Iron−Sulfur Proteins, Vol. I−III.*; Lovenberg, W., Ed.; Academic Press: New York, 1973−1977.
(3) *Iron−Sulfur Clusters, Vol. IV.*; Spiro, T. G., Ed.; John Wiley & Sons: New York, 1082.
(4) *Advances in Inorganic Chemistry, Vol. 38*; Cammack, R., Ed.: Academic Press: San Diego, 1992.
(5) Beinert, H.; Holm,; R. H.; Münck, E. *Science* **1997**, *277*, 653−659.
(6) Van Vleck, J. H. *The Theory of Electronic and Magnetic Susceptibilities*; Oxford University Press: 1966.
(7) Zener, C. *Phys. Rev.* **1951**, *82*, 403.
(8) Anderson, P. W.; Hasegawa, H. *Phys. Rev.* **1955**, *100*, 675−681.
(9) de Gennes, P.-G. *Phys. Rev.* **1960**, *118*, 141−154.
(10) Belinskii, M. I.; Tsukerblat, B. S.; Gerbeleu, N. V. *Sov. Phys. Solid State* **1983**, *25*, 497−498.
(11) Girerd, J.-J. *J. Chem. Phys.* **1983**, *79*, 1766−1775.
(12) Borshch, S. A. *Sov. Phys. Solid State* **1984**, *26*, 1142−1143.
(13) Papaefthymiou, V.; Girerd, J.-J.; Moura, I.; Moura, J. J. G.; Münck, E. *J. A. Chem. Soc.* **1987**, *109*, 4703−4710.
(14) Blondin, G.; Girerd, J.-J. *Chem. Rev.* **1990**, *90*, 1359−1376.
(15) Borras-Almenar, J. J.; Clemente-Juan, J. M.; Coronado, E.; Georges, R.; Palii, A. V.; Tsukerblat, B. S. *J. Chem. Phys.* **1996**, *105*, 6892−6909.
(16) Piepho, S. B.; Krausz, E. R.; Schatz, P. N. *J. Am. Chem. Soc.* **1978**, *100*, 2996−3005.
(17) Wong, K. Y.; Schatz, P. N. *Prog. Inorg. Chem.* **1981**, 369−449.
(18) Wong, K. Y. *Inorg. Chem.* **1984**, *23*, 1285−1290.
(19) Bersuker, I. B.; Borshch, S. A. In *Advances in Chemical Physics*; Prigogine, I., Rice, S. A., Eds.; John Wiley: New York, 1992; Vol. 81, pp 703−782.
(20) Borras-Almenar, J. J.; Clemente-Juan, J. M.; Coronado, E.; Palii, A. V.; Tsukerblat, B. S. In *Magnetoscience − From Molecules to Materials*; Miller, J., Drillon, M., Eds.; Willey-VCH: New York, 2001; pp 155−210.
(21) Borshch, S. A.; Chibotaru, L. F. *Chem. Phys.* **1989**, *135*, 375−380.
(22) Borshch, S. A.; Bominaar, E. L.; Blondin, G.; Girerd, J.-J. *J. Am. Chem. Soc.* **1993**, *115*, 5155−5168.
(23) Bominaar, E. L.; Borshch, S. A.; Girerd, J.-J. *J. Am. Chem. Soc.* **1994**, *116*, 5362−5372.
(24) Bominaar, E. L.; Hu, Z.; Münck, E.; Girerd, J.-J.; Borshch, S. A. *J. Am. Chem. Soc.* **1995**, *117*, 6976−6989.
(25) Noodleman, L.; Peng, C. Y.; Case, D. A.; Mouesca, J.-M. *Coord. Chem. Rev.* **1995**, *144*, 199−244.
(26) Glaser, T.; Rose, K.; Shadle, S. E.; Hedman, B.; Hodgson, K. O.; Solomon, E. I. *J. Am. Chem. Soc.* **2001**, *123*, 442−454.

ature (**2b)**; complete delocalization of electrons over three metal sites (**3b**) and finally complete electron delocalization via the magnetic core of the central metal site (**1b**). Thus, the last two compounds show electron delocalization over *all three* metal centers which is in line with the general expectation of smaller vibronic interactions in octahedrally coordinated low-spin iron complexes as compared to tetrahedral ones.[27]

In this paper, we present a theoretical description which explains the above properties as well as the total spin and the intervalence optical transitions of this new series of sulfur-bridged iron clusters. The detailed investigations made in ref 1 allowed us to derive a unifying minimal model based on the Hubbard Hamiltonian acting in the space of magnetic orbitals of metal sites. The one-electron parameters of this model, first of all the intersite electron transfer between magnetic orbitals, have been estimated from quantumchemical calculations. It was found that the relatively high value of the electron transfer between terminal iron sites, and especially its negative sign, play a crucial role in the electronic properties of these compounds, in particular, the strong ferromagnetic interaction in $[LFeCoFeL]^{3+}$, the ground-state spin $S = 1$ in $[LFeFeFeL]^{2+}$ and the vibronic valence trapping in $[LFeCoFeL]^{2+}$.

Model for Low-Lying Electronic States

We describe the lowest electronic states of our linear three metallic complexes by a simplified model involving the necessary minimal number of electronic configurations. By electronic configurations, we further mean particular population schemes irrespective to the spin directions of entering unpaired electrons (if any). A generally expected situation in the first row transition metal complexes is that the active molecular orbitals are of a 3*d* character,[28] although strong metal−ligand covalency can arise, especially, in Fe−S bonds.[29] This is also the case for $[LFeMFeL]^{n+}$ as the quantum chemistry calculations show. Then, the lowest electronic states are basically linear combinations of electronic configurations corresponding to different population schemes of these *d*-rich molecular orbitals.

To set up the minimal model for the low-lying electronic states we should first find the ground (i.e., the lowest in energy) electronic configuration. There are two ways to construct this configuration, following either the molecular orbital or the valence bond like approach. In the first case, the ground electronic configuration corresponds to the consecutive population of the lowest active molecular orbitals and therefore the gain of the covalent (electron delocalization) energy is maximal. However, the one-determinant electronic state constructed from molecular orbitals does not optimize the interelectron repulsion energy. This is achieved within the second approach which starts from the localized orbitals, generally of a broken symmetry type, obtained as linear combinations of active molecular orbitals. The coefficients in these linear combinations are found from the condition that the one-determinant state constructed from the localized orbitals minimizes the Coulomb repulsion between electrons occupying these orbitals. Actually, the minimal value of the interelectron repulsion is obtained by distributing the electrons occupying the active molecular orbitals over orbitals separated in space as well as possible. Because the active molecular orbitals are of a 3*d* character, the resulting localized orbitals will be centered on one of the metal ions, with admixtures of the orbitals of the ligands and of the other metals centers. In this picture, the localized orbitals occupied by unpaired electrons in the ground configuration are just magnetic orbitals introduced by Anderson in his theory of superexchange in magnetic insulators[30,31] and in later, more chemically oriented models.[32−34] Of course, the minimization of the electron repulsion energy in one-determinant approximation is achieved at the expense of covalent energy. Therefore, to choose the correct starting point we should compare the part of the covalent energy corresponding to electron delocalization between metal ions, expressed through the electron transfer parameters (resonance integrals) between orbitals localized at different metal centers, with the interelectron repulsion energy, mainly contributed by the Coulomb repulsion between the electrons occupying the same metal center (intracenter electron repulsion).

As it will be seen from further Extended Hückel calculations, the parameter of the electron transfer between neighbor metal centers, β, is of the order of 0.5 eV. The intracenter electron repulsion parameter, U, cannot be easily estimated from quantum chemistry calculations. Semiempirical estimations[30] give for U values in the range of 5−10 eV which are certainly larger than $|\beta|$ by an order of magnitude. Therefore the intracenter interactions are leading, so the ground and low-lying excited states will arise from electronic configurations corresponding to the lowest values of the intracenter electron repulsion energy at three metal ions. As an experimental evidence for this, the ground electronic configuration observed in $[LFeMFeL]^{n+}$ by various techniques[1] always corresponds to the minimal value of this energy.

Having established the ground electronic configuration (or configurations), the excited ones result from electron redistributions between the centers and either correspond to valence interchange (e.g., Fe(II)Cr(III) → Fe(III)Cr(II)) or to valence disproportionation (e.g., Fe(III)Cr(III) → Fe(II)Cr(IV)). An analysis based on bare metal ions (Appendix S1) shows that the excited configurations of the first (covalent) type are characterized by much lower excitation (electron promotion) energies than the configurations of the second (ionic) type. The ground electronic configuration and the excited covalent configurations form the ground manifold. In our approach, the low-lying electronic states arise just from this manifold of electronic configurations. The ionic configurations are much higher in energy and admix to the low-lying states in the second order after electron transfer.

Further calculations depend on the number of covalent configurations. If only one such configuration exists the electron transfer is quenched and the system is characterized by spin

(27) The change of the ionic radius under oxidation/reduction is determined by the contraction/expansion of the external 3*d* shell. The resulting forces acting on the ligands depend on the overlap of the 3d-orbital accommodating the migrating electron with the ligands orbitals. It is known that high spin complexes have more diffuse *d* orbitals as compared with isovalent low spin complexes which is manifested, for instance, in their larger ligand field splitting. Because the iron ion has high spin in tetrahedral and low spin in octahedral coordination one can expect larger vibronic coupling in the former case.

(28) Balhausen, C. J. *Introduction to Ligand Field Theory*; McGraw-Hill: New York, 1962.

(29) Glaser, T.; Hedman, B.; Hodgson, K. O.; Solomon, E. I. *Acc. Chem. Res.* **2000**, *33*, 859−868.

(30) Anderson, P. W. *Phys. Rev.* **1959**, *115*, 2−13.

(31) Anderson, P. W. In *Magnetism*; Rado, G. T., Suhl, H., Eds.; Academic Press: New York, 1963; Vol.1, Chapter 2, pp 25−83.

(32) Hay, P. J.; Thibeault, J. C.; Hoffmann, R. *J. Am. Chem. Soc.* **1975**, *97*, 4884−4899.

(33) Kahn, O.; Briat, B. *J. Chem. Soc., Faraday II* **1976**, *72*, 268; 1441.

(34) Girerd, J. J.; Journaux, Y.; Kahn, O. *Chem. Phys. Lett.* **1981**, *82*, 534.

Scheme 1

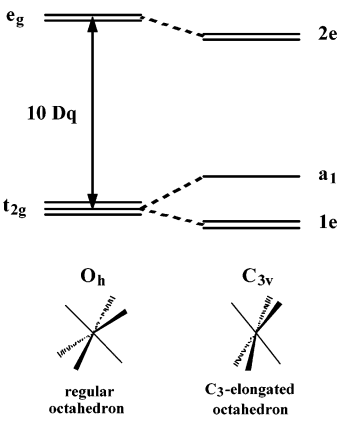

degrees of freedom only. This is clearly the case of conventional, "exchange" type complexes. By contrast, when the ground manifold involves several covalent configurations, these can be spanned by electron transfer interactions and the complex acquires both spin and charge degrees of freedom, i.e., it is of "mixed-valence" type. These two situations lead to a qualitatively different manifestation of the electron transfer in the magnetic properties of the compounds.[14,19]

An essential feature in the structure of the compounds under investigation is the existence of the trigonal symmetry with respect to the axis spanning the three metal ions, and of the inversion symmetry relative to the central metal (Chart 1). As a result the ligand field splitting of the *d*-orbitals at each metal ion acquires a trigonal component, as shown in Scheme 1 for terminal centers, where a_1 and e are the nondegenerate and 2-fold degenerate irreducible representation of the site symmetry group C_{3v}, respectively.[35] The central metal has a higher site symmetry, D_{3d}; therefore, the splitted *d* orbital should be characterized by irreducible representations of this group. For the sake of simplicity, we will not make use of them, since only the rotational C_3 symmetry is employed in further treatment. Due to this symmetry, allowing for degenerate orbital states, the relative order of the two lowest levels in Scheme 1 is very important for the magnetic properties of the complexes. In an ideal octahedral coordination, this order is one shown in Scheme 1 for the case of trigonal elongation, whereas it is reversed for the case of trigonal compression of the octahedron. Beside geometrical factors, the environment of each metal ion itself is pseudo-octahedral, which gives an additional contribution to the trigonal splitting. The order of localized orbitals at the three metal centers was established by spectroscopy (ref 1) and further clarified by quantum chemistry calculations.

Extended Hückel Calculations. The Extended Hückel calculations for the complex $[LFeFeFeL]^{2+}$ have been done using the CACAO package.[36] The geometrical parameters were taken from the crystal structure data[1]. The structure of this complex contains elongations of the pseudo-octahedral frames, N_3FeS_3 for terminal metal ions and S_3FeS_3 for the central ion, which are also present in other compounds of this series. There is a little deviation of the structure from the symmetry S_6 generated perhaps by counterions and crystal packing effects.

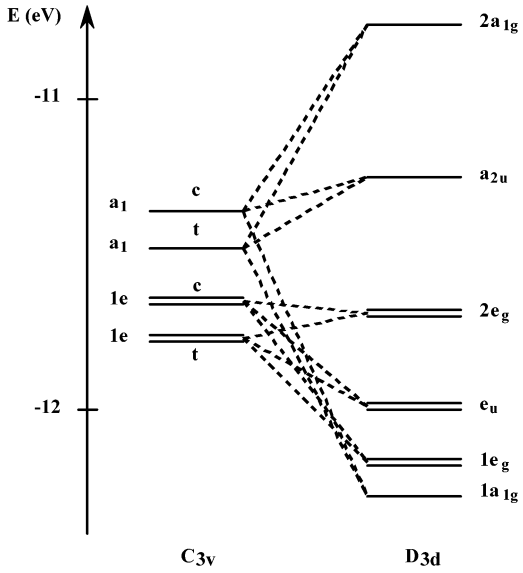

Figure 1. Energy levels correlation diagram between one-center orbitals (left side) and molecular orbitals (right side). The notations c and t stand for central and terminal fragments, respectively.

Scheme 2

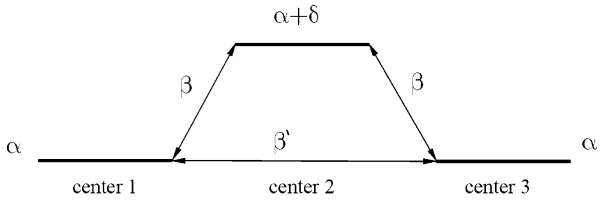

However, the molecular orbitals corresponding to the core $N_3FeS_3FeS_3FeN_3$, which are of primary interest here, are weakly subjected to low symmetry distortions: the splitting of the orbitals of *e* type amounts only several meV. We will neglect symmetry lowering effects in further discussions, using the core symmetry group D_{3d} and the fragment symmetry group C_{3v} for the characterization of the corresponding orbitals. The right-hand side of Figure 1 displays the energy levels of antibonding *d*-rich molecular orbitals. Essential hybridization of the sulfur orbitals observed for these MO arises from closed values of the ionization potentials for iron *d* and sulfur *p* orbitals. This reflects a general situation of stronger hybridization of sulfur orbitals in the Fe(*d*)-L bonding as compared with halogen and oxygen ligands.[31,29,37]

Evaluation of the One-Electron Model Parameters. In the simplest version of the model the one-electron part includes electron transfer processes only between orbitals localized at three metal centers which are partly occupied in the ground configurations. These correspond to components originating from the t_{2g} shell at each pseudo-octahedral metal center, i.e., to a_1 and 1*e* orbitals in Scheme 1. Because all three metal centers lie on the common symmetry axis the intercenter electron transfer is only possible between localized orbitals belonging to the same irreducible representation of the trigonal group, a_1, e_x, or e_y. This is shown in Scheme 2 for one such orbital per center. β denotes the transfer parameter between the terminal (1, 3) and the central (2) ions; β' is the transfer parameter between terminal ions; α and $\alpha + \delta$ are orbital energies of the

(35) Cotton, F. A. *Chemical Applications of Group Theory*; Wiley-Interscience: New York, 1990; 3rd ed.
(36) Mealli, C.; Prosperio, D. M. *J. Chem. Education* **1990**, *67*, 399.
(37) Gamelin, D. R.; Bominaar, E. L.; Kirk, M. L.; Wieghardt, K.; Solomon, E. I. *J. Am. Chem. Soc.* **1996**, *118*, 8085−8097.

Scheme 3

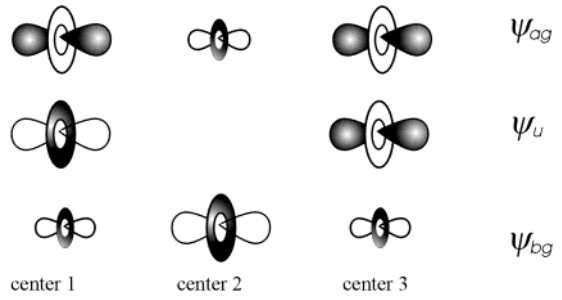

terminal and central ions, respectively. The corresponding Hückel type Hamiltonian reads as follows

$$H_t = \beta(t_{12} + t_{23}) + \beta' t_{13} + \alpha(n_1 + n_3) + (\alpha + \delta)n_2 \quad (1)$$

in which the operator t_{ij} is defined by its action on the orbital ϕ_i and ϕ_j at corresponding centers

$$t_{ij}\phi_i = \phi_j, \qquad t_{ij}\phi_j = \phi_i$$

while n_i is the occupation operator, giving the number of electrons of both directions of spin in the corresponding orbital. The eigenvalue problem for H_t is simplified by using symmetrized combination of localized orbitals

$$\psi_u = \frac{1}{\sqrt{2}}(\phi_1 - \phi_3), \quad \psi_{1g} = \frac{1}{\sqrt{2}}(\phi_1 + \phi_3), \quad \psi_{2g} = \phi_2 \quad (2)$$

where the subscripts u and g in the left-hand side are parity indices. The above combinations hold for each type of localized one-center orbitals (a_1, $1e_x$, and $1e_y$), all being of even parity with respect to the inversion. Because there is only one odd function in the basis set (2), it already corresponds to an eigenfunction of (1). The other eigenfunctions are linear combinations of the even functions

$$\psi_{bg} = c_1\psi_{1g} + c_2\psi_{2g}$$

$$\psi_{ag} = c_2\psi_{1g} - c_1\psi_{2g}$$

$$c_1^2 + c_2^2 = 1 \quad (3)$$

where the subscript b and a denotes the bonding and antibonding orbital, respectively. The resulting eigenvalues are

$$\epsilon_{bg} = \alpha + \frac{1}{2}[\delta + \beta' - \sqrt{8\beta^2 + (\delta - \beta')^2}]$$

$$\epsilon_{ag} = \alpha + \frac{1}{2}[\delta + \beta' + \sqrt{8\beta^2 + (\delta - \beta')^2}]$$

$$\epsilon_u = \alpha - \beta' \quad (4)$$

Note that the obtained energy levels depend on the sign of β' and do not depend on the sign of β. The latter only affects the relative sign of the coefficients c_1 and c_2 in (3). Scheme 3 shows the corresponding eigenfunctions and the symmetry indices corresponding to the D_{3d} group for the case of $a_1(d_z^2)$ localized orbitals at metal centers and $\beta < 0$.

The transfer parameters entering eq 1 can be estimated by equating the eigenvalues in eq 4 with the energies of the *d*-rich molecular orbitals appropriate by symmetry (Figure 1).[38] Actually we must perform a unitary transformation from the calculated molecular orbitals (right-hand side of Figure 1) to one-center localized orbitals (left-hand side of Figure 1). Due to the common rotational axis, this transformation will connect only localized and molecular orbitals of the same symmetry as indicated by dashed lines in the middle of Figure 1. This means that one can obtain the model parameters by fitting the energy expressions (4) to each group of three molecular orbitals with the same symmetry index, a_1, $1e_x$, $1e_y$, the last two being equivalent by symmetry. However we face the problem that three energy levels in eq 4 cannot unequivocally determine four parameters of the model, α, δ, β, and β'. Such complications always arise when one is trying to obtain localized orbitals from a set of molecular orbitals transforming after repeating irreducible representations[41] (the case for the two gerade orbitals in Scheme 3). This means that we cannot resort on symmetry relations connecting the localized orbitals, like in the case of metal centers equivalent by symmetry, and the only way to find the coefficients of the unitary transformation toward localized orbitals, and the model parameters in eq 1, is to perform the minimization of the Coulomb repulsion between electrons occupying the molecular orbitals as it was discussed above. Such a calculation, however, is far beyond the Extended Hückel approach. Nevertheless we can still obtain an estimate for the transfer parameters supposing negligible values of δ. In this case, the three parameters, α, β and β' are easily found from the three equations (4). The results are quoted in the first two columns of the Table 1. A better estimation could be expected from an approach modeling the localized orbitals by fragment EH calculations at each metal center. The fragment calculations for terminal and central iron ions in the nearest neighbor environments, N_3FeS_3 and S_3FeS_3 respectively, were performed using again the CACAO package. The resulting lowest *d*-rich levels are shown in Scheme S1. Equating the energy difference between the orbitals of the central and terminal fragments of the same symmetry in Scheme S1 with δ, one can use again the equations (4) to find another three one-electron parameters for orbitals of each symmetry type. The results are shown in the last two columns of Table 1. The quality of this type of

Table 1. One-Electron Model Parameters Derived from EH Calculations (in eV)

	equivalent centers ($\delta = 0$)		nonequivalent centers	
	a_1	$1e$	a_1	$1e$
α	−11.430	−11.936	−11.472	−11.976
δ			0.125	0.122
$\lvert\beta\rvert$	0.534	0.168	0.523	0.159
β'	−0.184	0.008	−0.226	−0.032

(38) Note that this is just an estimation. The transfer parameters entering (1) and the effective Hamiltonian (7) include implicitly also the contribution of the interactions of the chosen configurations with another ones, not included in the model space. For instance, the electron transfer from the orbitals $1e$ of one center to the excited orbitals $2e$ (Scheme 1) of another center is allowed by symmetry and will contribute to the parameters β and β' in the second order of perturbation theory. An exact evaluation of the model parameters is possible by combining model approach with high level quantum chemistry calculations of the lowest states.[39,40] However, the renormalization of the transfer parameters with respect to the proposed estimations is not expected to be strong in our case.

(39) Ceulemans, A.; Chibotaru, L. F.; Heylen, G. A.; Pierloot, K.; Vanquickenborne, L. G. *Chem. Rev.* **2000**, *100*, 787−805.
(40) Calzado, C. J.; Cabrero, J.; Malrieu, J. P.; Caballol, R. *J. Chem. Phys.* **2002**, *116*, 2728−2747; 3985−4000.
(41) Kahn, O. *Molecular Magnetism*; VCH Publishers: New York, 1993.

estimations can be assessed from the calculated ratios of the transfer parameters for a_1 and 1e orbitals in trigonal titanium dimers by Extended Hückel[42] and CASSF[43] methods, which show good agreement.

One can see from Table 1 that the nondegenerate localized orbital a_1 lies higher in energy for both terminal and central ions (Scheme 1). This result is in agreement with the conclusion drawn from Mössbauer investigations of these compounds[1], which have shown that such an order of the lowest localized orbitals at the metal centers is a common feature for all complexes under investigation.[44] The same orbital order can be expected also from a simple ligand field argument (see the discussion above) although the π-bonding effects may influence the trigonal splitting. The electron-transfer parameters for nearest neighbor sites is several times stronger for a_1 orbitals than for the orbitals 1e. The former are mainly composed from d_z^2 orbitals aligned to the common C_3 axis (Scheme 3), which produces their strong through-space overlap.[43] However the ratio of the β parameters for a_1 and e orbitals is not as large as, for instance, in $[Ti_2Cl_9]^{3-}$ dimers,[43] where it amounts -6.5, which is explained by a stronger covalency of the Fe−S than of the Ti−Cl bonds in the e-type molecular orbitals of the corresponding compounds. A surprising result is the obtained appreciable value of the elecron transfer between terminal orbitals a_1, which is caused by their nonnegligible overlap. It will be seen below that the transfer parameter β', and especially its sign, plays a crucial role in the magnetic properties of the compounds.

Model Hamiltonian. The localized orbitals 1e in Scheme 1 are filled on all iron and cobalt ions in the ground configuration of the complexes. Because the electron transfer operator (1) connects localized orbitals of the same symmetry, only the configurations arising from the repopulation of a_1 orbitals between three centers can admix in the ground manifold. As for the chromium ion, it contains a half filled 1e shell. Nevertheless it will be shown that the lowest states in [LFeCrFeL]$^{n+}$ mainly arise from the repopulations of the a_1 orbitals in the ground manifold also. Therefore the minimal model can be formulated in the space of a_1 orbitals only.

As it was discussed above the main interaction in the space of localized orbitals is due to the intracenter electron repulsion

$$H_U = U_1(n_{1\uparrow}n_{1\downarrow} + n_{3\uparrow}n_{3\downarrow}) + U_2 n_{2\uparrow}n_{2\downarrow} \qquad (5)$$

where $n_{i\uparrow}$ and $n_{i\downarrow}$ are occupation operators of the a_1 orbital for spin up and spin down electrons at the three metal sites and U_i are the corresponding electron repulsion parameters ($U_1 = U_3$) having values of 5−10 eV. Next in the order of importance is the intercenter electron repulsion

$$H_K = K(n_1n_2 + n_2n_3) + K'n_1n_3 \qquad (6)$$

where K and K' are electron repulsion parameters for nearest neighbor and terminal sites respectively with the order of magnitude of 1−2 eV. Finally, the one-electron part H_t in eq 1, corresponding to electron transfer between a_1 orbitals, should be included. This operator contains transfer parameters which do not exceed 0.5 eV.

Scheme 4

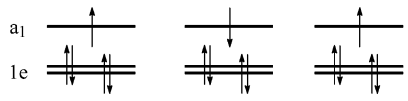

Scheme 5

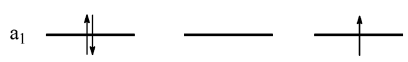

The three contributions in eqs 5, 6, and 1 describe the main interactions in the space of a_1 orbitals. The resulting Hamiltonian

$$H = H_U + H_K + H_t \qquad (7)$$

corresponds to a version of the extended Hubbard model[45] and will be further applied to all complexes under investigation.

Results and Discussion

[LFeFeFeL]$^{3+}$. The lowest value of the electron repulsion energy in eqs 5 and 6, $2K + K'$, is achieved for a single configuration shown in Scheme 4. This is in line with the Mössbauer data[1] testifying about the trivalent state of each iron ion in this compound. The resulting two $S = 1/2$ and one $S = 3/2$ spin states are degenerate because they are inactive for the one-electron operator (1), except for its diagonal part, which has the same value, $3\alpha + \delta$, for all three states. To remove this degeneracy we should involve the ionic configurations which can admix via electron transfer. There are six ionic configurations resulting from the redistribution of a single electron in the ground configuration (Scheme 5). The bielectronic energies of these configuration are $U + 2K$ and $U + 2K'$ ($U \equiv U_1 \approx U_2$) and all of them correspond to $S = 1/2$.

In the absence of the electron transfer ($\beta = \beta' = 0$), the ionic and covalent spin states form two degenerate manifolds separated roughly by U (left-hand side of Figure 2).[41] It can be seen from Scheme 5, that the electron transfer operator can connect different ionic states thus lifting their degeneracy. When only the transfer between nearest neighbor ions is taken into account the ionic states split into three levels coinciding with the three straight lines on Figure 2. These are still degenerate after parity. The interaction between covalent and ionic states via electron transfer results in their further splitting. Thus, the even covalent spin state $S = 1/2$ interacts with the second even spin state from the ionic manifold (3^2A_{1g}), whereas the odd one interacts with the first and third odd ionic states in Figure 2 (2^2A_{2u} and 4^2A_{2u}, respectively). At the same time, the single spin state with $S = 3/2$ will rest unaffected by this interaction. Hence the ground state spin corresponds to the experimentally observed $S = 1/2$. The only effect of the electron transfer between terminal centers on the covalent spin states, not included in this consideration, is the lowering of the energy of the first excited level 1^2A_{1g}.

The above picture is greatly simplified if one takes into account the relation between the parameters, $|\beta|/U \ll 1$, which

(42) Leunberger, B.; Güdel, H. U. *Mol. Phys.* **1984**, *51*, 1−20.
(43) Ceulemans, A.; Heylen, G. A.; Chibotaru, L. F.; Maes, T. L.; Pierloot, K.; Ribbing, C.; Vanquickenborne, L. G. *Inorg. Chim. Acta* **1996**, *251*, 15−27.
(44) The method used in ref 1 is based on the observation that for a d^5 low spin system in trigonal symmetry, the contributions of the valence electrons to the electric field gradient at the metal nucleus are respectively positive and negative for the configurations $(1e)^4(a_1)^1$ and $(a_1)^2(1e)^3$. Therefore, the sign of the measured quadrupole splitting gives already the order of the occupied localized orbitals at the corresponding metal center. This sign was found positive for all Fe(III) sites in the seven compounds [LFeMFeL]$^{n+}$ (see Table 5 in ref 1).
(45) Fulde, P. *Electron Correlations in Molecules and Solids*; Springer Ser. in Solid-State Sciences, Cardona, M., et al., Eds.; 1995; Vol. 100.

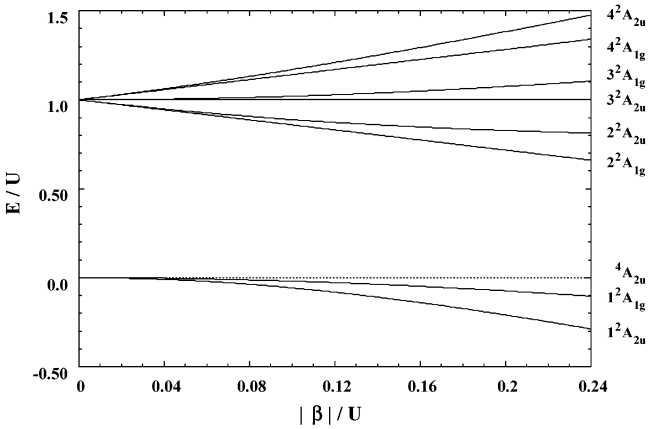

Figure 2. Spectrum of the electronic states for $[LFeFeFeL]^{3+}$ as function of the transfer parameter β in the case $\beta' = 0$. Solid lines correspond to $S = 1/2$ and the dotted line to $S = 3/2$. The energy of the ground configuration (Scheme 4) was taken as zero of energy.

Scheme 6

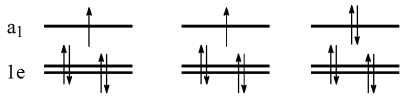

was stressed in the previous section. In this case, the relative positions of the low-lying levels are described by second-order terms after β, β' and can be reproduced by the Heisenberg Hamiltonian for localized spins $S = 1/2$ at the centers

$$H = -2J_a(\vec{S}_1\vec{S}_2 + \vec{S}_2\vec{S}_3) - 2J_t\vec{S}_1\vec{S}_3 \qquad (8)$$

with the following exchange parameters ($\delta \approx 0$)

$$J_a = -\left(\frac{\beta^2}{U - 2K + K'} + \frac{\beta^2}{U - K'}\right), \quad J_t = -\frac{2\beta'^2}{U - K'} \qquad (9)$$

These are, of course, particular cases of antiferromagnetic kinetic contributions to the superexchange interaction.[30,31,41] Note that ferromagnetic contributions corresponding to direct (potential) exchange interaction[30] are generally augmented to the exchange parameters in eq 9, resulting in the diminishing of their negative values. This effect, however, is expected to be weak as compared to the antiferromagnetic effect because of appreciable values of transfer parameters β and β' (Table 1). Magnetic susceptibility measurements have shown[1] that only the $S = 1/2$ ground-state spin is populated even at room temperature which, according to simulations of $\mu_{\text{eff}}(T)$in ref 1, implies $-J_a + J_t > 400$ cm^{-1}. This gives the estimation $|\beta| > 0.5$ eV for $U - K = 10$ eV[30] which fits well into the data of Table 1.

$[LFeFeFeL]^{2+}$: Two Particle Model. The electronic configuration with the minimal electron repulsion energy, $U + 3K + 2K'$, is the one shown in Scheme 6, in agreement with Mössbauer studies.[1] Indeed, the last show an almost equal delocalization of the excess electron over all centers, whereas in linear three nuclear clusters this can only occur when the energy of a localized electron is lower on terminal ions than on the central ion. Because of the inversion symmetry of the compound, there exists two equivalent ground configurations of this type, corresponding to the localization of the pair of electrons in the $a_1$orbital of one of the terminal iron sites. The configuration with two electrons on the central ion (Scheme 7) has a close value of the electron repulsion energy, $U + 4K + K'$, because it merely corresponds to valence interchange between two nearest iron centers. Thus there are three covalent configurations in the ground manifold with the same valence distribution 2Fe(III) + Fe(II).

Scheme 7

Scheme 8

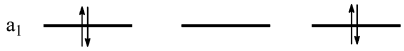

Within our model, we have to describe a system of four electrons in three orbitals. This situation is equivalent with the consideration of two holes (see the Appendix). The essential point is the change of the signs of all one-electron parameters in eq 1. Each covalent configuration is equivalent with the location of the holes on a given pair of centers, resulting in two spin states, $S = 0,1$. The symmetrized combination of these states are described by the following wave functions Ψ^S for $S = 1$ ($M_S = S$)

$$\Psi^1_{A_1g} = |\psi_{1g}\psi_{2g}|$$

$$\Psi^1_{1A_2u} = |\psi_u\psi_{1g}|$$

$$\Psi^1_{2A_2u} = |\psi_u\psi_{2g}| \qquad (10a)$$

and for $S = 0$

$$\Psi^0_{A_2u} = \frac{1}{\sqrt{2}}(|\psi_u\bar{\psi}_{2g} - |\bar{\psi}_u\psi_{2g}|)$$

$$\Psi^0_{1A_1g} = \frac{1}{\sqrt{2}}(|\psi_{1g}\bar{\psi}_{1g}| - |\psi_u\bar{\psi}_u|)$$

$$\Psi^0_{2A_1g} = \frac{1}{\sqrt{2}}(|\psi_{1g}\bar{\psi}_{2g}| - |\bar{\psi}_{1g}\psi_{2g}|) \qquad (10b)$$

where the symmetrized orbitals ψ are defined in eq 2 but now correspond to holes; A_{1g} and A_{2u} in the subscripts of the left-hand side are one-dimensional irreducible representations of the group D_{3d}, whereas the numbers in front denote repeating representations. There are also three ionic configurations, one of them being represented in Scheme 8. They all correspond to $S = 0$. In the absence of electron (hole) transfer the covalent and ionic states form two degenerate manifolds separated approximately by U as it is shown in the left-hand side of Figure 3. We neglected for the sake of simplicity the energy differences between electronic configurations generated by geometrical nonequivalency of the centers whose effect on the covalent states will be considered later.[46] It results from Schemes 6−8 that the ionic configurations cannot be transposed into each other by the transfer of one electron while the covalent configurations can.

Consider first the effect of nearest neighbors electron transfer on these two manifolds separately. The three ionic states will remain degenerate. The covalent states will split with β into three levels, coinciding with three solid lines in Figure 3, which

(46) Beside K and K', for the sake of simplicity we neglect here also the effects of δ and β' on the splitting of the ionic states, which are not important for the spectrum of low-lying spin states when U is large.

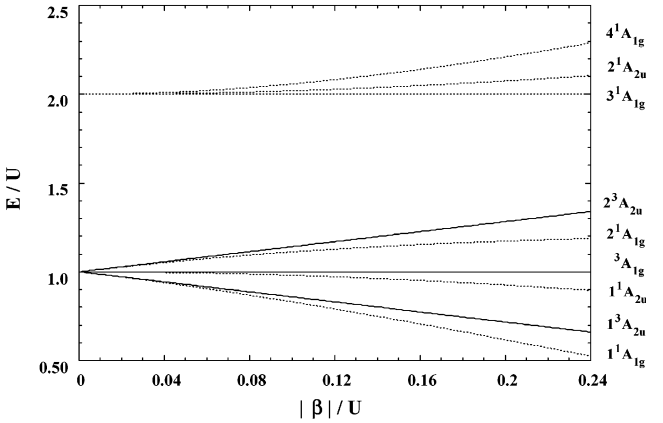

Figure 3. Same as in Figure 2 for the case of $[LFeFeFeL]^{2+}$. Solid and dotted lines correspond to $S = 1$ and $S = 0$ states, respectively.

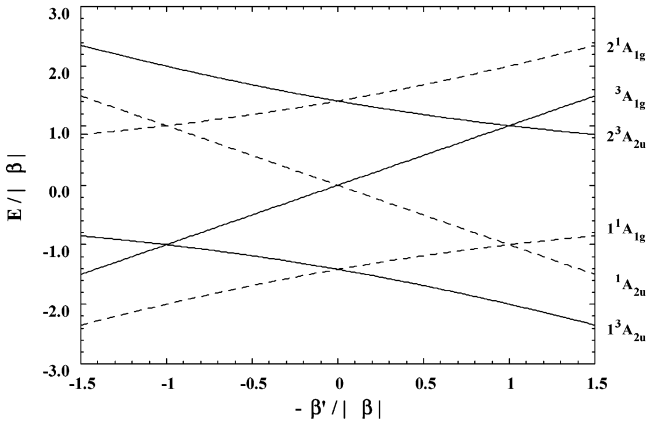

Figure 4. Energy levels of the covalent states of $[LFeFeFeL]^{2+}$ as functions of β' for the case $\Delta = 0$. Solid and dashed lines correspond to $S = 1$ and $S = 0$ states, respectively.

are still degenerate after spin. This accidental degeneracy is not removed when the energy difference between covalent configurations is taken into account. The interaction between covalent and ionic states via electron transfer leads to the mutual repulsion of the levels of the same spin and parity. This lifts the degeneracy of the levels in the second order after β/U as it is shown in Figure 3. Note the opposite behavior of the covalent and ionic states as function of β in $[LFeFeFeL]^{3+}$.

The obtained picture of energy levels in Figure 3 does not depend on the sign of the parameter β. It results, hence, that the ground state is always a spin singlet, which particularly is not the case for $[LFeFeFeL]^{2+}$ where the ground state with $S = 1$ has been found. This is the consequence of an oversimplified consideration of the transfer interaction, which did not involve the electron (hole) transfer between terminal centers. The last influences the covalent states already in the first order of the perturbation theory after the parameter β', which, according to Table 1, is apparently larger than the expected splitting $3\beta^2/U$ between the two lowest covalent states in Figure 3.[47] More accurate description of the covalent states is obtained by the diagonalization of the Hamiltonian (A.1), taking into account $\beta' \neq 0$, in the space of the wave functions (10). The obtained energy levels (A.2) are shown in Figure 4 as functions of $\beta'/|\beta|$ for the case $\Delta = 0$. We can see that the degeneracy of the covalent states after spin in the absence of the interaction with ionic states is removed already in the first order after β', the relative order of the obtained levels with $S = 0$ and $S = 1$ depending on its sign. The ground-state spin $S = 1$ is obtained for $\beta' < 0$. The last relation matches our estimation of β' for $[LFeFeFeL]^{n+}$ complexes (Table 1).

As one can see from Figure 4 the picture of energy levels corresponding to the two-particle model is symmetric against the interchange of $S = 0$ and $S = 1$ multiplets and the concomitant change of the sign of β'. The origin for this is investigated in detail in the Appendix S2. This specific symmetry becomes transparent when we investigate the matrix of the transfer Hamiltonian in the form given by eq B4. In particular, the form (B4) of this matrix implies a linear component in the dependence of the eigenvalues on the transfer parameters. Thus, the linear dependence of the singlet−triplet splitting emerges when all three transfer parameters are different from zero in contrast to the situation met in the exchange complex $[LFeFeFeL]^{3+}$. Finally, one general aspect of the two-particle model is worth mentioning. Being applied to the case of two electrons instead of two holes, it will give the same results for the opposite sign of β'. Both two-hole and two-electron cases are examples of situations when one particle is added to a background with one spin $S = 1/2$ per site. This situation is close to the one described by the double exchange model.[7,8] In this model, to gain kinetic energy the delocalizing particles try to align the localized spins of the metal ion cores via the Hund's rule coupling, which leads to the ferromagnetic ground state. A similar picture is supported by the Nagaoka theorem[48] which states that a simple lattice of spins 1/2 becomes ferromagnetic when one electron or hole is added. Therefore, one can expect at first glance the ferromagnetic ground state in our case also. In this view, the result obtained above, that the ground state can be either singlet or triplet depending on the sign of β', seems to be counterintuitive. Actually, the double exchange model does not fit perfectly into the two-particle model because in the latter case the orbitals containing background spins and the delocalized particle are not separated but belong to the same orbital space. On the other hand, the Nagaoka theorem does not apply for the one-dimensional case (chains) where the Lieb−Mattis theorem[49] predicts the singlet ground state. Both of these theorems, however, are formulated for infinite systems and their extrapolation to clusters should be done with caution.

Returning to the complex $[LFeFeFeL]^{2+}$, note that the above model is not very realistic in that it did not take into account the difference between the centers. The effect of this difference, described by the parameter Δ in eq A.3 , can be expected to be of the same order of magnitude as the transfer parameters. The energy levels expressions taking into account the effect of Δ are quoted in eq A.2 and their dependence on β' is shown in Figure 5. One can see that there are no qualitative differences between the obtained energy spectra in Figures 4 and 5. The main effect of Δ is to shift the group of two levels in the middle of the spectrum toward the lowest group of levels. At the same time Δ increases the splitting between the lowest levels.

The observed intervalence band in the IR spectra of $[LFeFeFeL]^{2+}$ (ref 1) should be assigned to the transition

(47) Although the origin of this splitting is the same as in the previous compound of "exchange" type, $[LFeFeFeL]^{3+}$, the obtained covalent states cannot be described by a traditional exchange Hamiltonian (8), because of several configurations involved in the ground manifold.

(48) Nagaoka, Y. *Phys. Rev* **1966**, *147*, 392.
(49) Lieb, E.; Mattis, D. *Phys. Rev.* **1962**, *125*, 164.

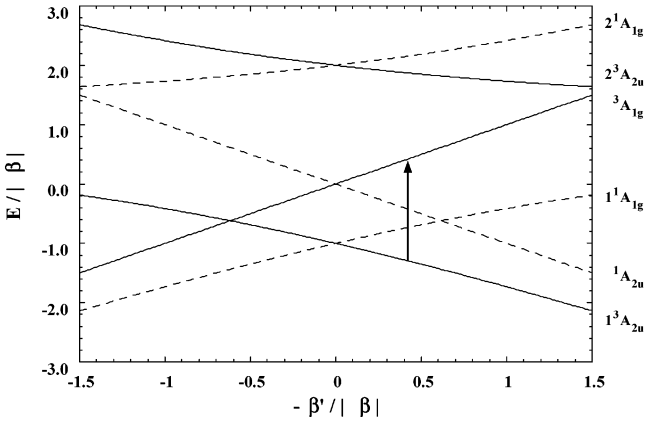

Figure 5. Same as in Figure 4 for the case $\Delta/|\beta| = 1$. The vertical arrow indicates the intervalence transition.

Scheme 9

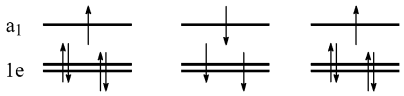

between the ground and a single excited state with $S = 1$ of a different parity, $^3A_{1g}$. As it results from eq A.2, the energy of this transition, $E^1_{A_1g} - E^1_{lA_2u}$, increases with $|\beta|$, $-\beta'$ and diminishes with increasing Δ. For the estimations of the transfer parameters in Table 1, $|\beta| \approx 0.5$ eV, $-\beta'/|\beta| \approx 1/3$, the observed energy of this transition, 0.7 eV, is achieved in our model at $\Delta/|\beta| \approx 1.5$, which looks quite reasonable. For these parameters, the triplet−singlet gap has the value $E^0_{lA_1g} - E^1_{lA_2u} = 0.4$ eV.

Having solved the problem for covalent states, we should include their interaction with ionic states. Since the latter correspond to $S = 0$, the main effect of this interaction is pushing down the lowest spin singlet in Figures 4 and 5. The resulting energy stabilization of this singlet (of the order β^2/U) is not strong enough to change the order of the lowest states whose splitting was obtained already in the first order after β'. Therefore, the triplet−singlet splitting will remain large compared to the conventional exchange interaction between localized spins. This is confirmed by magnetic susceptibility measurements[1] for $[LFeFeFeL]^{2+}$ showing no populatiuon of other spin states beside the ground one up to room temperature.

$[LFeCrFeL]^{3+}$. The trigonal splitting of the localized orbitals at the metal centers was estimated to be not very large (see Table 1), so that the fulfilement of the Hund rule for the electrons within the t_{2g} shell of the chromium center can be expected. Then, the electron configuration corresponding to the minimal electron repulsion energy is the one in Scheme 9, which is in line with Mössbauer data[1]. Therefore, as in the case of $[LFeFeFeL]^{3+}$, there exists one single ground-state configuration all other being ionic. However now the electron transfer between all types of localized orbitals (a_1, $1e_x$ and $1e_y$) can change the ground configuration. The estimation of the transfer parameters in Table 1 yields $\beta_e^2/\beta_a^2 \approx 0.1$, which means that we can neglect the effect of electron transfer between degenerate orbitals on the stabilization of the states from the ground manifold. Therefore, the only relevant ionic configurations are those arising from the ground configuration by electron redistributions between a_1 orbitals of three centers. These are just the ionic configurations involved in the case of $[LFeFeFeL]^{3+}$, one of them being represented on Scheme 5.

Three electrons occupying the orbitals a_1, $1e_x$, and $1e_y$ on the cromium center and interacting via Hund rule coupling give the total spin of this ion $S = 3/2$ in the ground state. Clearly, the low-lying electronic states of the complex will correspond to the Hund states on the chromium center. There is also a set of spin states arising from the ground configuration with non-Hund spin states $S = 1/2$ on the chromium ion. Although these states lie much lower in energy than the ionic states, they cannot admix directly to the Hund states. The contributions of the non-Hund states to the stabilization of the Hund states via electron-transfer begin with the forth order of perturbation after β, β'. Therefore, we can neglect the non-Hund states in the further consideration.

The covalent configuration from Scheme 9, with the Hund state on chromium center, results in one $S = 5/2$, two $S = 3/2$, and one $S = 1/2$ spin states. The one-electron transfer can mix them only with ionic states which are also of Hund type, i.e., correspond to maximal possible spin on the chromium ion. Indeed, the chromium spin state $S = 3/2$ in the ground manifold is a sum of the spin $S = 1$ of two electrons in the orbitals $1e_x$ and $1e_y$ and the spin $S = 1/2$ of one electron in the a_1 orbital. The transfer of an additional electron on or the removal of a single electron from the chromium a_1 orbital will not change the spin state of the $1e$ shell, resulting in $S = 1$ state of the chromium center. However, the back transfer of one electron from the double occupied or on the empty a_1 orbital of the chromium ion will not convert it automatically into the initial $S = 3/2$ state. The overall situation of the interaction between covalent and ionic states through electron transfer is shown in Scheme S2.

Further calculations are performed in complete analogy with the $[LFeFeFeL]^{3+}$ case. In the second order of perturbation theory the relative position of the four levels from the ground manifold are described by the Heisenberg Hamiltonian, eq 8, for localized spins $S_1 = S_3 = 1/2$, $S_3 = 3/2$ with the following exchange parameters

$$J_a = -\frac{1}{3}\left(\frac{\beta^2}{U_2 - K' + \delta} + \frac{\beta^2}{U_1 - 2K + K' - \delta}\right),$$

$$J_t = -\frac{2\beta'^2}{U_1 - K'} \qquad (11)$$

where δ is the energy difference for a_1 magnetic orbitals on the chromium and iron ions and U_2 and U_1 are the corresponding intrasite electron repulsion parameters, eq 5. Both exchange parameters in eq 11 correspond to antiferromagnetic coupling between the centers. Because according to our estimations $\beta^2 > 3\beta'^2$, the obvious relation $|J_a| > |J_t|$ takes place. Hence, the order of the spin states is $E(1/2) < E(3/2) < E(5/2)$, in agreement with experiment[1]. From magnetic susceptibility measurements the exchange parameters $J_a = -130$ cm^{-1} and $J_t = -50$ cm^{-1} were derived. The obtained large value of the antiferromagnetic exchange between terminal centers is not surprising in view of large value of β'. Indeed, replacing the denominators in eq 11 by an average U we obtain for the ratio J_t/J_a an approximate value $3\beta'^2/\beta^2$. For our estimation $|\beta'/\beta| \approx 1/3$ in Table 1 we obtain $J_t/J_a = 0.33$, which compares well with the experimental ratio 0.38. Taking the values of transfer parameters from the first column in Table 1, we reproduce the experimental J_t for

Scheme 10

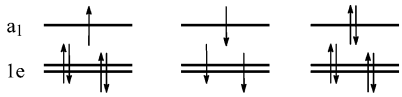

Scheme 11

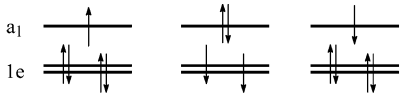

$U_1 - K' = 10$ eV in the second equation of (11), which value fits perfectly the Anderson's estimation for pairs of Fe(III) ions.[30] At the same time the experimental J_a is reproduced for an average value of 11.5 eV for denominators in the first equation of (11). This last value seems to be exagerated since the repulsion parameter for chromium, U_2, is expected to be smaller than for a three valent iron.[30] One of the reasons for that is our neglect of other, ferromagnetic contributions to the exchange interaction. These are the ferromagnetic kinetic[50] and the direct exchange contributions. The first one involves electron transfer from filled 1*e* orbitals of iron to half-filled 1*e* orbitals of chromium and also from them to the empty 2*e* orbitals of iron (Scheme 1). This contribution is expected to be small due to small values of transfer parameters between degenerate orbitals (Table 1). By contrast, the direct ferromagnetic exchange between chromium and iron ions can be important since, compared to the antiferromagnetic contribution in eq 11, it does not contain the statistical factor 1/3. Another reason for the above descrepancy could be an exaggerated values of β since our estimations of the transfer parameters in the previous section referred to $[LFeFeFeL]^{n+}$ complexes.

$[LFeCrFeL]^{2+}$: Spin Dependent Delocalization. The reduced form of the previous compound, given the higher orbital energy on chromium than on iron, has the ground configuration of the type indicated on Scheme 10, which is again in line with experiment.[1] Due to the inversion symmetry there is also another equivalent configuration, corresponding to the double occupation of the a_1 orbital on the opposite center. The configuration in Scheme 11 occurs from the previous ones by valence interchange between neighbor centers, so it belongs to the ground manifold as well. Therefore, as in the case of $[LFeFeFeL]^{2+}$, there are three covalent configurations in the ground manifold but now we have to consider the problem of six electrons. As before, to simplify this problem we pass to the representation of holes, which permits to reduce the number of particles to four. In this representation, the configurations in Scheme 10 and Scheme 11 become as in Schemes S3 and S4 correspondingly. The problem is further simplified by neglecting the electron (hole) transfer between 1*e* orbitals on the same grounds as for the previous complex. Hence, we come at last to the problem of two particles moving in the space of a_1 orbitals, similar to one considered for $[LFeFeFeL]^{2+}$. The new feature is that the delocalization of these two particles takes place in the presence of a magnetic core, arising from the common spin of two unpaired electrons from the 1*e* orbitals of the chromium ion.

The low-lying states we are looking for correspond to Hund states of the chromium ion as it was the case for $[LFeCrFeL]^{3+}$.

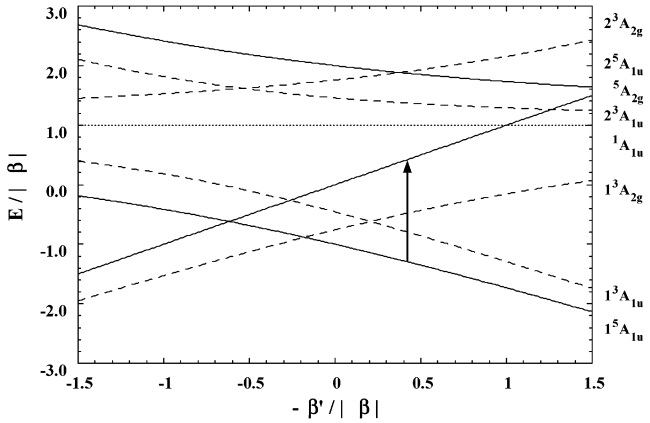

Figure 6. Energy levels of covalent states of $[LFeCrFeL]^{2+}$ as functions of β' for the case $\Delta/|\beta| = 1$. Solid lines denote $S = 2$ states, dashed lines correspond to $S = 1$ states and the dotted line to the $S = 0$ state.The vertical arrow indicates the intervalence transition.

Thus, the problem is confined by the states with $S = 3/2$ on the chromium ion for the case of configurations in Scheme 10 and the states with $S = 1$ on the chromium ion, for the case of the configuration in Scheme 11. The basis for the eigenvalue problem involves two $S = 2$ and two $S = 1$ states of both even and odd parity, coming from the configurations in Scheme 10, together with one odd $S = 2$ state, two $S = 1$ states of both parities and one $S = 0$ state coming from the configuration in Scheme 11. The appropriate Hamiltonian should include additional terms in eq A.1 describing the exchange interactions of unpaired electrons in the chromium ion. Because all the states involved in the eigenvalue problem are of Hund type, the new terms will merely lead to an unimportant energy shift of $3J$ for all resulting eigenstates, where J is the parameter of the exchange interaction for the chromium t_{2g} shell. The energies of the obtained low-lying states are given in eq A.4 and their dependence on β' is shown in Figure 6 for $\Delta > 0$. We can see that the ground-state spin is $S = 2$ in accordance with the experimentally observed[1]. Although one can expect that the sign of the parameter β' is not changed when passing from Fe−Fe−Fe to Fe−Cr−Fe systems, its negative sign is not already necessary to achieve the ground state with the maximal spin, as it was the case in $[LFeFeFeL]^{2+}$. In the case $\Delta = 0$ (Figure S2) the ground spin $S = 2$ is preserved for zero and even for positive values of β', unless $\beta' \geq |\beta|/\sqrt{15}$. As Figure 6 shows, this situation is not changed qualitatively when the difference between the iron and chromium centers, described by the parameter Δ, is taken into account.

To understand the different behavior of low-lying states for $[LFeFeFeL]^{2+}$ and $[LFeCrFeL]^{2+}$ we should examine the energy expressions in eq A.4. Their main difference from the corresponding expressions in eq A.2 resides in the state dependent factors in front of β^2. Accordingly, one can speak about an effective nearest neighbor transfer parameter, which is β for odd $S = 2$ states, $\sqrt{2/3}\beta$ for even $S = 1$ states and $\sqrt{1/3}\beta$ for odd $S = 1$ states. This is the larger value of the effective transfer parameter for $S = 2$ states which determines the resulting stabilization of this spin in the ground state of $[LFeCrFeL]^{2+}$. Thus, we face here the phenomenon of spin dependent electron delocalization induced by the magnetic core of the chromium ion. Because of a single magnetic core, our problem is similar to the Kondo problem of electrons scattered by magnetic

(50) Goodenough, J. B. *Magnetism and Chemical Bond*; Interscience: New York, 1963, Chapter 5.

Scheme 12

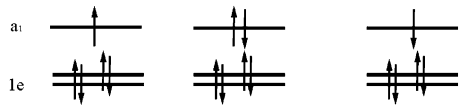

impurities in crystals[51,45] rather than to the double exchange. Indeed, the dependence of the electron delocalization on the total spin is not of a double exchange type as proven in Appendix S3.

The observed intervalence band in the IR spectrum of $[LFeCrFeL]^{2+}$ is assigned to the transition to the $^5A_{2g}$ state (vertical arrow in Figure 6), the only one allowed by symmetry. In the limit of large Δ we obtain from (A4) for the energy of this transition

$$E^2_{A_2g} - E^2_{lA_1u} \approx -2\beta' + \frac{2\beta^2}{\Delta} \qquad (12)$$

The second term in this equation is much smaller than the first one, which according to our estimations ins in Table 1, $-2\beta' = 0.37$ eV, already matches the experimental transition energy, 0.42 eV. Δ has therefore a value of several eV's. The difference from the intervalence transition in $[LFeFeFeL]^{2+}$, which has the same dependence on the parameters (compare eqs (A2) for $S = 1$ states with eq A4 for S = 2 states), is that Δ was obtained much lower for that complex.

For small values of $|\beta'|$, the lowest excited state is 1^3A_{2g}, intersected then by 1^3A_{1u} at larger $|\beta'|$, Figure 6. For large values of Δ 1^3A_{1u} will be the lowest excited state given the estimated ratio $|\beta'/\beta| \approx 1/3$. Using eq A4, in the limit of large Δ we obtain for the quinted-triplet separation

$$E_{QT} = E^1_{lA_1u} - E^2_{lA_1u} \approx \frac{4}{3}\frac{\beta^2}{\Delta} \qquad (13)$$

The interaction of 1^3A_{1u} with a single ionic state appropriate by symmetry (corresponding to a combination of configurations with two holes on one or another iron ions) stabilizes it by 4/3 β^2/U, and to the same extent is reduced E_{QT}. Note that this correction is of the same order as E_{QT} itself, eq 13. The gap is further reduced by the interaction of the lowest triplet with non-Hund triplet states, which stabilize it in the fourth order after hole transfer, and due to the vibronic interaction between the lowest excited triplet states discussed below. As a result the gap can be small or even change the sign. This is in agreement with the observed quintet-triplet gap of $\sim$100 cm^{-1}. By contrast, in $[LFeFeFeL]^{2+}$ the triplet−singlet gap remain large for any values of Δ, as it follows from (A2). Therefore, it cannot be efficiently reduced by other effects.

Reducing this complex further results in $[LFeCrFeL]^{+}$ with one single hole distributed over a_1 orbitals of three centers. A similar theoretical analysis (Appendix S4) gives the spin $S = 3/2$ of the ground state, in accordance with experiment[1], and the itinerant hole almost localized at the chromium center.

$[LFeCoFeL]^{3+}$. It results from Mössbauer data that the ground electronic configuration in this compound is the one shown in Scheme 12. It has the same population of a_1 orbitals as the excited covalent configuration of $[LFeFeFeL]^{2+}$ in Scheme 7. Because the cobalt and iron ions are in the same three valent state any electron redistribution in the ground configuration will lead to valence disproportionation between centers, i.e., to ionic configurations. There are three types of such configurations. The transfer of a single electron from the cobalt center results in two equivalent configurations as in Scheme 6. In our model, the electron promotion energy corresponds to $-\Delta$, where Δ is given by eq A3. However now δ itself is negative and has a large value, of the order of U, the same is expected for (now negative) Δ. The next excited ionic configurations are those shown in Scheme 13, i.e., corresponding to one electron redistribution between terminal iron centers. Finally, the highest in energy will be the configuration in Scheme 8 because it corresponds to maximal valence disproportionation, Fe(III)Co(III)Fe(III) → Fe(II)Co(V)Fe(II). We will investigate consequently the effect of ionic configurations of the first two types on the lowest spin states.

Scheme 13

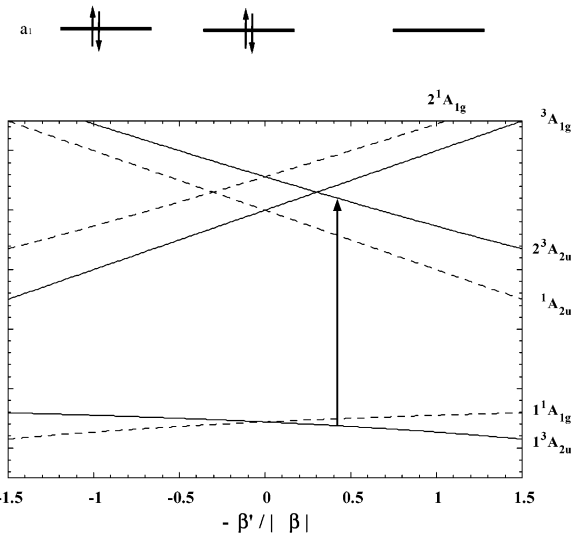

Figure 7. Energy levels of the covalent states of $[LFeCoFeL]^{3+}$ as functions of β' for the case $\Delta/|\beta| = -3$. Solid and dashed lines correspond to $S = 1$ and $S = 0$ states, respectively. The vertical arrow indicates the expected intervalence transition.

The admixture of the states arising from the lowest excited configurations in Scheme 6 can be considered within the two particle model employed for $[LFeFeFeL]^{2+}$. The only difference from that case is the change of the sign of Δ, which is negative now. The low-lying states are described by the expressions (A.2), in which the zero of energy corresponds to the configuration in Scheme 6. The resulting energy levels diagram is shown in Figure 7. We can see that as in the case of $[LFeFeFeL]^{2+}$ the ground-state spin is obtained $S = 1$ for $-\beta' > 0$ and $S = 0$ otherwise. Again, as in the former complex, the sign of β' in Table 1 favors the spin triplet ground state in accordance with experiment. The triplet−singlet gap decreases with increasing Δ but much faster than it was found for the quintet triplet gap in $[LFeCrFeL]^{2+}$, eq 13. It can be described as resulting from the exchange interaction between two spins $S = 1/2$ localized at terminal iron centers. The corresponding exchange parameter is obtained from eq A2 in the limit of large $|\Delta|$ as follows

$$J_f = \frac{1}{2}(E^0_{lA_1g} - E^1_{lA_2u}) \approx -\frac{2\beta^2\beta'}{\Delta^2} \qquad (14)$$

(51) Kondo, J. *Prog. Theor. Phys. (Kyoto)* **1964**, *32*, 37.

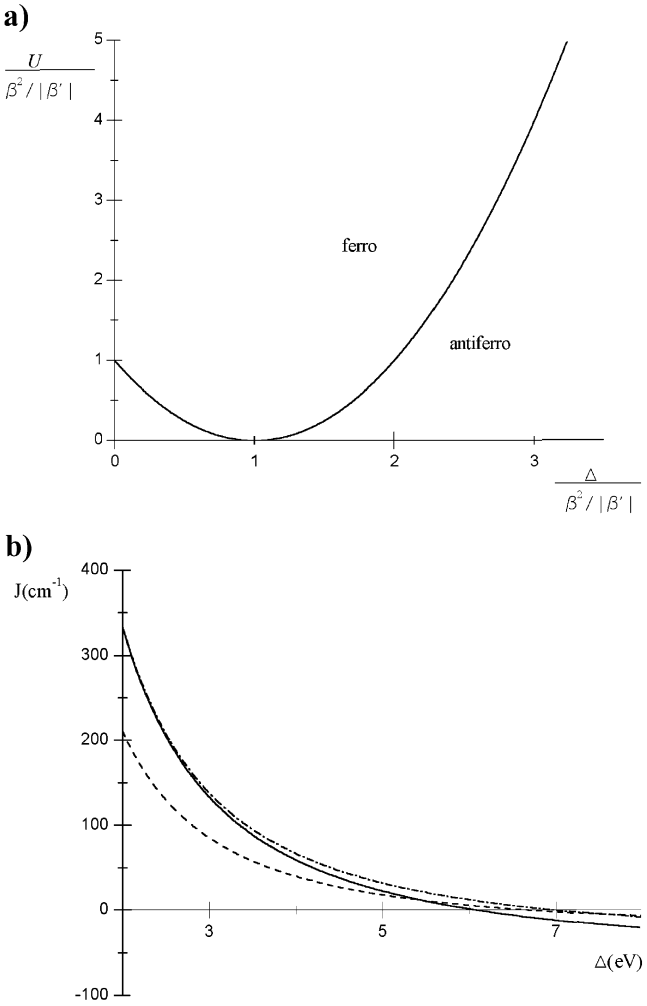

Figure 8. (a) The exchange interaction described by the joint contributions in eqs 19 and 20 as function of U and Δ. (b) The exchange parameter in $[LFeCoFeL]^{3+}$ for $-\beta'/|\beta| = 1/3$ and $\beta = 0.5$ eV, $U = 10$ eV (dash−dotted line); $\beta = 0.4$ eV, $U = 10$ eV (dashed line); $\beta = 0.5$ eV, $U = 7$ eV (solid line).

Consider now the admixture of the states from the configuration in Scheme 13. Its main effect consists of the stabilization of the obtained spin singlet states. We mentioned above that this kind of admixture was unable to change the spin of the ground state in $[LFeFeFeL]^{2+}$. In the present case, the situation is different because of a small value of the triplet−singlet splitting in eq 14. The interaction of the lowest singlet state 1^1A_{1g} with the ionic state appropriate by symmetry (corresponding to a symmetric combination of two configurations as in Scheme 13) results in its stabilization and, therefore, leads to an antiferromagnetic contribution to the gap described by the exchange parameter (in the limit of large U_1 and Δ)

$$J_a = -\frac{2\left(\frac{\beta^2}{\Delta} + \beta'\right)^2}{U_1 - K'} \qquad (15)$$

The final exchange parameter, corresponding to the second term in eq 8, is the sum of the above contributions, $J_t = J_f + J_a$. This can generally be either ferromagnetic or antiferromagnetic depending on the interplay between Δ and $U \equiv U_1 - K'$ as it is shown in Figure 8a. However, as Figure 8b shows, the resulting interaction will be always ferromagnetic if realistic parameters, appropriate to $[LFeCoFeL]^{3+}$ are used.

Scheme 14

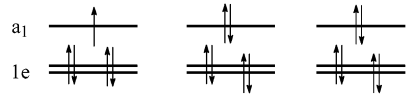

Scheme 15

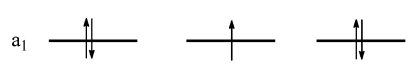

The contribution J_a in (15) has a transparent physical meaning. It is nothing but antiferomagnmetic kinetic exchange arising due to electron transfer between magnetic orbitals localized at terminal centers (cf eq 9). The effective transfer parameter (the expression in the brackets) consists of two contributions: the direct transfer (β') and the indirect one, via the localized orbital of the central cobalt ion (β^2/Δ). These contributions partially cancel in the case of negative β'. By contrast the contribution J_f in (14) is not conventional albeit it has the same kinetic origin. It is easily checked[52] that the right-hand side of eq 14 is a third-order perturbation expression involving three steps of electron transfer along two equivalent paths. These paths involve the transfer of an electron from the cobalt ion to one of the terminal iron ions (β), to the opposite iron ion (β') and then back to the central ion (β). Since this process involves only one step of electron transfer between terminal ions, the corresponding contribution to the exchange depends on its sign. Therefore, one can conclude that the ferromagnetic exchange interaction found[1] in $[LFeCoFeL]^{3+}$ ($J_t = 42$ cm^{-1}) is due to the negative sign of β'.

The only allowed optical transition from the ground state is shown in Figure 7 by a vertical arrow. It results from eq (A.2) that the energy of this transition is

$$E^1_{A_1g} - E^1_{lA_2u} \approx |\Delta| + |\beta'| + \frac{2\beta^2}{|\Delta|} \qquad (16)$$

i.e., it increases with $|\Delta|$, which is opposite to the situation in $[LFeFeFeL]^{2+}$ and $[LFeCrFeL]^{2+}$. Therefore, we can expect the location of the corresponding transition at much higher energy than in the latter cases, of several eV's. This is corroborated by the experimental observation that no intervalence band was detected below 1100 nm in $[LFeCoFeL]^{3+}$. In the higher energy region (210−1100 nm), no intervalence band was assigned due to the spectral interference with strong charge-transfer transitions[1].

$[LFeCoFeL]^{2+}$: Vibronic Valence Trapping. It follows from the analysis of the low-temperature Mössbauer spectrum that there are two equivalent ground configurations in this compound, one of which is shown in Scheme 14. Beside these, a single excited configuration exists, which corresponds to the location of an unpaired electron on the cobalt center (Scheme 15). In the representation of holes the picture is reduced to one single particle moving over three a_1 orbitals. The resulting electronic states merely correspond to molecular orbitals in eq 3, now for holes, with the energies as in eq 4.[53] Note that the

(52) Landau, L. D.; Lifshitz, E. M. *Quantum Mechanics*; Pergamon: Oxford, 1975, 2nd ed.

(53) These are obtained from electronic molecular orbital energies (4) by changing the signs of all one-electron parameters. Following the convention adopted for the zero of energy in eq A.2 we should put $\alpha = 0$ in eq 4.

parameter δ from these energy expressions should be replaced by Δ, which has the same form as in the case of $[LFeCrFeL]^+$ (Appendix S4).

In contrast to the previous compounds a new feature arises in the temperature dependence of the Mössbauer spectrum of $[LFeCoFeL]^{2+}$. At low temperature, the spectrum shows a superposition of signals from Fe^{2+} and Fe^{3+}, which is consistent with the localization of the unpaired electron on the one of terminal iron centers. Increasing the temperature a new line appears which can be attributed to intermediate valence $Fe^{2.5}$ of the iron ions[1]. This clearly points on the temperature induced localization-delocalization transition in the compound. On the other hand all three electronic states of the complex correspond to an equal delocalization of the unpaired electron (hole) over both iron centers as eqs 2 and 3 show. The additional interactions, leading to the trapping of the unpaired electron at low temperatures, are provided by the relaxation of the ligand shells upon addition of this electron in the corresponding localized states (vibronic interactions). Such interactions have been found to be responsible for valence trapping in mixed valence compounds.[14,19−24]

The vibronic problem for linear mixed-valence trimers with one delocalizing particle has been already unvestigated.[54] In the case of $[LFeCoFeL]^{2+}$ complex this problem effectively reduces to the case of a dimer. Indeed, due to the relation $\beta \ll \Delta$, the lowest electronic states in $[LFeCoFeL]^{2+}$ mainly correspond to the delocalization of the hole between terminal centers only. The effective transfer parameter corresponding to this delocalization is obtained from the perturabation theory as

$$t = -\beta' - \beta^2/\Delta \tag{17}$$

which obviously coincides with the corresponding transfer amplitude for the previous compound (cf eq 15). The relaxation of the ligand shell upon addition of the excess hole in a localized a_1 state of one of the terminal iron ions is accounted for by the electron-vibrational interaction term

$$H_{ev} = \lambda(Q_1 n_1 + Q_3 n_3) \tag{18}$$

where λ is the vibronic coupling parameter independent of spin, the coordinates Q_i measure a symmetric local distortion around corresponding centers $i = 1,3$, and n_i are hole occupation operators. It is convenient to pass from Q_i to symmetrized coordinates

$$Q_+ = \frac{1}{\sqrt{2}}(Q_1 + Q_3)$$

$$Q_- = \frac{1}{\sqrt{2}}(Q_1 - Q_3) \tag{19}$$

of even and odd symmetry with respect to the inversion. H_{ev} can be rewritten as

$$H_{ev} = \lambda\left[\frac{1}{\sqrt{2}}Q_+ + \frac{1}{\sqrt{2}}Q_-(n_1 - n_3)\right] \tag{20}$$

To obtain the potential energy surface, the elastic energy of nuclear vibrations $1/2k(Q_1^2 + Q_3^2)$, where k is the force constant of the metal−ligand bond assumed to be independent from the oxidation state, should be added. With the transformation (19) this energy reads

$$E_{el} = \frac{1}{2}k(Q_+^2 + Q_-^2) \tag{21}$$

The interaction with the vibration Q_+ is identical for all electronic states and therefore will lead to the same relaxation energy, $\Delta E(Q_+) = -\lambda^2/4k$. On the other hand the interaction with Q_- is described by the operator $n_1 - n_3$ which can mix electronic states of different parity, leading to broken symmetry solutions corresponding to the localization of the excess hole on one of the two terminal centers. To find this out, we should diagonalize the electronic Hamiltonian, describing the bonding and the antiboding hole orbitals, spaced by $2|t|$ (Scheme 16), together with the interaction matrix in eq 20, and then investigate the lowest energy eigenvalue as function of Q_-.

Scheme 16

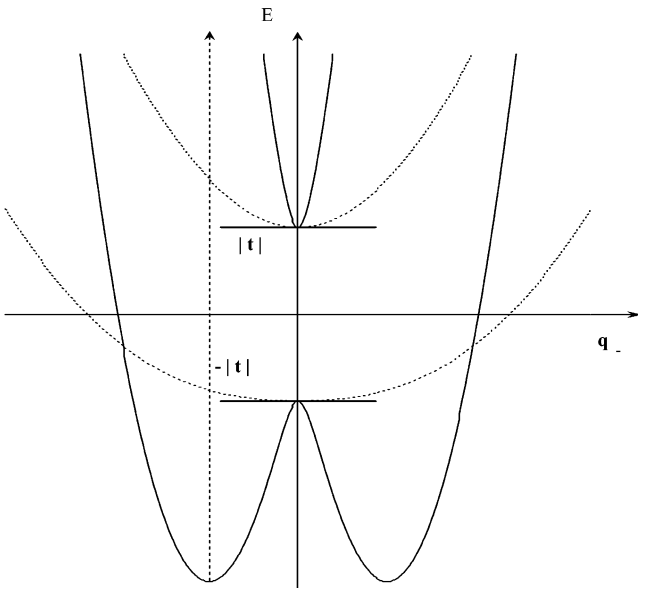

The resulting energy surface is well-known for mixed valence dimers.[14,19] For small vibronic coupling parameters the lowest energy surface is close to a parabolic function of Q_-. However, when the relation between parameters

$$|t| < \frac{\lambda^2}{2k} \tag{22}$$

is valid the lowest energy surface becomes of a two-well type (Scheme 16), the two symmetric minima corresponding to the localization of the excess particle at one of the two centers. The dashed lines in Scheme 16 correspond to potential curves in the absence of vibronic interaction and the continuous lines show their transformation in the case when the relation (22) is fulfilled. This relation has a simple physical meaning. The left-hand side is the energy gain due to the hole delocalization between two centers, whereas the right-hand side is the relaxation energy with respect to a local distortion when the hole is localized on one of the centers.

The energy of the intervalence transition also depends on the relation (22). It corresponds to $2|t|$, the spacing between two one-particle levels in the dimer at $Q_- = 0$, when this relation

(54) Bersuker, I. B.; Borshch, S. A.; Chibotaru, L. F. *Chem. Phys*. **1989**, *136*, 379−385.

is not satisfied, and to λ^2/k otherwise.[14,19] In the last case the intervalence transition takes place from the bottom of one of the two minima with $Q_- \neq 0$ on the lowest energy surface (shown by a vertical arrow in Scheme 16). In the complex $[LFeCoFeL]^{2+}$ the intervalence transition was found at 0.76 eV, which means, in view of the fulfillement of (22), that the effective transfer parameter is $|t| < 0.38$. This is in line with our estimations of transfer parameters β,β' in Table 1, the more that the two contributions in eq 17 partially cancel due to the negative sign of β'.

We should note that vibronic valence trapping can be in principle expected in $[LFeFeFeL]^{2+}$ and $[LFeCrFeL]^{2+}$ too, which are mixed valence compounds as well. However there is no evidence for that in Mössbauer spectra. To investigate the possibility of vibronic valence localization in the ground state of these compounds we consider first the limit of large Δ which, as in the case of $[LFeCoFeL]^{2+}$, reduces the problem to the case of a dimer. The electronic state which can admix to the ground state via vibronic interaction is just the one involved in the intervalence transition in these compounds (Figures 5 and 6, respectively). Taking half of the corresponding energy of the transition, eq 12, we obtain for the effective transfer parameters between terminal iron ions in both compounds

$$t = \beta' - \beta^2/\Delta \tag{23}$$

which is different from (17) because both contributions now add to each other for negative β'. The reason for the sign change in front of β' in eq 23 is that in $[LFeFeFeL]^{2+}$ and $[LFeCrFeL]^{2+}$ an electron instead of a hole is effectively transferred between terminal centers in the highest spin state. This is clearly seen from the electronic configurations in Schemes 6, 7 and Schemes 10, 11 for the two complexes, respectively.

In the case of $[LFeFeFeL]^{2+}$, the limit of large Δ is hardly realized because it does not fit the experimental intervalence transition. In this case, the vibronic treatment should involve the effects of ligand shell relaxation around all three centers by adding a third nuclear coordinate Q_2 corresponding to the central ion. However, the electron (hole) trapping will be described again by one odd coordinate Q_-, the second equation in (19), because the other two symmetrized coordinates are of even parity.[54] The criterion for structural instability with respect to this coordinate, corresponding to valence trapping at one of the terminal centers, is obtained after some algebra in the form

$$E_{IV} < \frac{\lambda^2}{k}(c_0)^2 \tag{24}$$

In this equation, E_{IV} is the energy of the intervalence transition observed in a given compound and c_0 is the coefficient with which the combination of the lowest configurations (Scheme 6 for $[LFeFeFeL]^{2+}$ and Scheme 10 for $[LFeCrFeL]^{2+}$) is contained in the ground-state wave function. The coefficient c_0 is unity in the limit when the excited covalent configuration (Scheme 7 and Scheme 11 for the two compounds, respectively) is not admixed to the ground state (Δ is large) when the problem reduces to a dimer case considered above. In the opposite case of full delocalization ($\Delta = 0$), we obtain $c_0 \approx 0.71$.

In $[LFeFeFeL]^{2+}$, we have estimated $\Delta/|\beta| = 1.5$ which gives $c_0 = 0.88$ for the ratio $-\beta'/|\beta| = 1/3$ (Table 1). Taking for λ^2/k the same value as in $[LFeCoFeL]^{2+}$ (i.e., the corresponding $E_{IV} = 0.76$ eV) we obtain for the right-hand side of (24) the value 0.59 eV, which is smaller than the left-hand side, $E_{IV} = 0.69$ eV. This means that the relation (24) is not fulfilled for $[LFeFeFeL]^{2+}$, and therefore, the vibronic valence trapping does not occur in this compound. At the same time, the vibronic interaction leads to the repulsion of the lowest two singlet levels (of different parity) close to their intersection point (Figure 5), which contributes to the stabilization of the lowest singlet 1^1A_{1g}. However, the triplet−singlet gap still remains too large to be efficiently reduced by interaction with ionic states as calculations show.

For the above value of Δ and c_0, the population numbers of the configurations in Schemes 6 and 7, corresponding to localization of the excess electron on one of the three centers, is 0.38, 0.24, and 0.38. On the other hand, Mössbauer studies seem to indicate a more even electron distribution. An equal distribution of the excess electron density among the centers arises in our model for $\Delta - \beta' = |\beta|$ ($c_0 \approx 0.82$), i.e., at a lower value of $\Delta/|\beta|$ compared to the estimation resulting from the fitting of intervalence transition. Although it is not possible to obtain population numbers for electron configurations directly from Mössbauer spectra, we note that the estimated value $|\Delta|/|\beta| = 1.5$ refers to a rigid scheme of levels in Figure 5. The calculations taking into account vibronic effects show that, due to a different relaxation of the 1^3A_{2u} and 1^3A_{1g} states (Figure 5) after totally symmetric nuclear coordinates Q_+, eq 19, and Q_2, the fitting of the intervalence transition is achieved at lower values of $\Delta/|\beta|$.

In $[LFeCrFeL]^{2+}$, the situation is entirely different. Given the small energy of intervalence transition ($E_{IV} = 0.42$ eV), the relation (24) is not valid for any positive Δ. Since vibronic valence trapping is not seen in $[LFeCrFeL]^{2+}$, the only reason for this discrepancy could be a smaller value of vibronic coupling parameter λ as compared to the $[LFeCoFeL]^{2+}$ complex, leading to an almost twice reduced λ^2/k for expected large values of Δ. Whatever the strength of vibronic coupling, it leads to the repulsion between the lowest singlet states 1^3A_{1u} and 1^3A_{2g} close to their intersection (Figure 6), which results in an efficient reduction of the quintet-triplet gap in eq 13.

Conclusions

In this study, we have shown that the properties of the ground and low-lying excited electronic states in the isostructural series of heterotrinuclear thiophenolate-bridged complexes $[LFeMFeL]^{n+}$ with M = Cr, Co, and Fe can be successfully described within a simple model approach supported by experiment (ref 1) and quantum chemistry calculations. The approach includes the electron transfer between magnetic orbitals at different metal centers, described by transfer parameters (Hückel-like resonance integrals between magnetic orbitals), and the electron repulsion in these orbitals and corresponds to a version of Hubbard model. Depending on valences included, it reduces to Heisenberg, $t-J$, or Kondo-like models for the lowest excited states. The unifying role of the Hubbard model is manifested also in the approximate invariance of the transfer and repulsion parameters within the series of compounds (the only parameter which changes drastically is the energy difference between localized orbitals at the central and terminal metal ions). Due to the trigonal symmetry of the complexes, only the electron transfer between nondegenerate orbitals, a_1, originating from the t_{2g} shell of each

metal ion in a pseudo-octahedral coordination, is relevant for the lowest states. Despite its simplicity, this three-orbital description is able to reproduce the observed ground and lowest excited spin states and the magnitude of the excitation energy, the electron delocalization and the intervalence transition in all investigated complexes.

An essential feature resulting from quantum chemistry calculations is the surprisingly large value and the negative sign of the electron transfer between terminal iron ions, β'. This feature allows to explain the unusual magnetic properties found in these compounds: the strong antiferromagnetic interaction between terminal ions in $[LFeCrFeL]^{3+}$, the spin ground state $S = 1$ and the large spin gap in $[LFeFeFeL]^{2+}$, and finally, the spin $S = 1$ and strong ferromagnetic interaction between terminal metal ions in $[LFeCoFeL]^{3+}$. In the complex $[LFeFeFeL]^{2+}$ the obtained ground state spin is only due to the negative sign of β' and would be $S = 0$ for opposite sign. Despite the fact that this complex and $[LFeCrFeL]^{2+}$ show spin-dependent delocalization, this cannot be attributed to the double exchange. The strong ferromagnetism between distant spins in $[LFeCoFeL]^{3+}$ arises from a three-step kinetic mechanism, apparently not discussed before, involving the electron transfer between terminal iron ions with corresponding parameter of negative sign as one of the steps. The vibronic valence trapping in the complex $[LFeCoFeL]^{2+}$ results from a reduced electron transfer between terminal iron centers, which is due to the negative β' and high promotion energy of electron transfer from cobalt to iron ions. In $[LFeFeFeL]^{2+}$ and $[LFeCrFeL]^{2+}$, the vibronic interaction between first and second excited states is expected to result in vibronic valence trapping in the lowest excited state and to reduce the excitation energy from the ground state. Vibronic valence trapping in the excited state of $[LFeCrFeL]^{2+}$ could be detected in the temperature-dependent Mössbauer spectra as a temperature induced delocalization−localization transition.

To conclude, the present investigation shows that the combination of a model approach with quantum chemistry and detailed experiment can be very efficient in providing insight into various magnetochemical problems. The original advance of the proposed approach is the use of simple quantum chemistry calculations to set up adequate physical models for low-lying states. This is especially important in cases when neither ab initio nor DFT methods can be successfully applied. Besides, the model description is valuable on its own because it provides the ultimate reason for the observed properties, as resulting from the interplay of several basic interactions.[39,40] A nice illustration for that is the new kinetic mechanism of strong ferromagnetic interaction between distant spins found in the present study. Finally, with realistic estimations of the parameters the adequate microscopic models prove well suited also for the prediction of electronic properties of isostructural compounds. From this perspective, the proposed theoretical approach gives a practical tool for both description and understanding of electronic and magnetic properties of polynuclear complexes which is accessible for magnetochemists.

Acknowledgment. We thank Dr. Laurent Petitjean for his help with quntum chemistry calculations. L.F.C. acknowledges financial support by the Belgian National Science Foundation and Flemish Government under the Concerted Action Scheme, and the visiting grant (poste PAST du Ministère de l'Education) to Orsay where this work was initiated.

Supporting Information Available: Appendicies S1−S4, containing electron promotion energies in bare metal ions, the analysis of the symmetry of two-particle model used for **3b**, the investigation of the origin of spin-dependent delocalization in **1b**, and the model study of the magnetism and electron delocalization in **1a**, respectively; Table S1, Figures S1−S4 and Schemes S1−S9, quoted in appendicies and in the main text. The material is available free of charge via the Internet at http://pubs.acs.org.

Appendix

Two Particle Model. Passing from electrons to holes merely changes the sign of all one-electron matrix elements, so we have to add a minus in front of transfer parameters and one-center orbital energies. The Hamiltonian describing the covalent states from the ground manifold is obtained as follows

$$H = C - \beta(t_{12} + t_{23}) - \beta' t_{13} - (\alpha + U_1 + 2K + 2K') \times (n_1 + n_3) - (\alpha + \delta + U_2 + 4K)n_2 + K(n_1 n_2 + n_2 n_3) + K' n_1 n_3 \quad \text{(A1)}$$

where the constant C is the electronic energy of filled a_1 orbitals on three metal centers. Note that the intracenter electron repulsion can affect the relative energies of covalent states only via the difference between U_1 and U_2, that is why the Hubbard term, eq 5, is not contained explicitly in (A1). The above Hamiltonian is actually obtained by applying the projector P, which restricts the space of functions to covalent states from the ground manifold, to the whole Hamiltonian (7), PHP.[14] Therefore, it is completely analogic to the kinetic term of the $t - J$ model widely applied in solid-state physics.[45]

The matrix of the Hamiltonian (A1) written in the basis of wave functions (10) is easily diaigonalized because the only nonzero off-diagonal matrix elements arise between the states $\Psi^1_{1A_2u}$, $\Psi^1_{2A_2u}$ and $\Psi^0_{1A_1g}$, $\Psi^0_{2A_1g}$, respectively. The resulting energies (E^S) are listed in eq A2

$$\begin{aligned}
E^1_{A_1g} &= -\beta' \\
E^1_{lA_2u} &= \frac{1}{2}\Delta + \frac{1}{2}\beta' - \sqrt{2\beta^2 + (\Delta - \beta')^2/4} \\
E^1_{hA_2u} &= \frac{1}{2}\Delta + \frac{1}{2}\beta' + \sqrt{2\beta^2 + (\Delta - \beta')^2/4} \\
E^0_{A_2u} &= \beta' \\
E^0_{lA_1g} &= \frac{1}{2}\Delta - \frac{1}{2}\beta' - \sqrt{2\beta^2 + (\Delta + \beta')^2/4} \\
E^0_{hA_1g} &= \frac{1}{2}\Delta - \frac{1}{2}\beta' + \sqrt{2\beta^2 + (\Delta + \beta')^2/4}
\end{aligned} \quad \text{(A2)}$$

where the energy of the ground electronic configuration of $[LFeFeFeL]^{2+}$ (Scheme 6) was taken as zero of energy and the subscribes l and h in the left-hand side stand for the lowest and the highest level of a given symmetry and spin. The parameter

$$\Delta = \delta + (K - K') + (U_2 - U_1) \quad \text{(A3)}$$

describes the energy difference between the excited and the ground covalent configurations shown in Schemes 7 and 8, respectively. As it was mentioned, δ and $U_2 - U_1$ are expected to be small in $[LFeFeFeL]^{n+}$ complexes.

Spin Dependent Delocalization. The Hamiltonian describing the delocalizing holes in the a_1 orbitals of $[LFeCrFeL]^{2+}$ is given by the same expression, eq (A1), as in the case of $[LFeFeFeL]^{2+}$. The magnetic interaction between localized and itinerant holes on the chromium ion will not affect the relative order of the low lying states, provided the space of covalent Hund states is only considered. Within this basis set, the eigenvalue problem is reduced to the diagonalization of three 2×2 matrixes corresponding to odd $S = 2$ states, even $S = 1$ states and odd $S = 1$ states. The resulting energies (E^S) are as follows

$$E^2_{A_2g} = -\beta'$$

$$E^2_{lA_1u} = \frac{1}{2}\Delta + \frac{1}{2}\beta' - \sqrt{2\beta^2 + (\Delta - \beta')^2/4}$$

$$E^2_{hA_1u} = \frac{1}{2}\Delta + \frac{1}{2}\beta' + \sqrt{2\beta^2 + (\Delta - \beta')^2/4}$$

$$E^1_{lA_2g} = \frac{1}{2}\Delta - \frac{1}{2}\beta' - \sqrt{(4/3)\beta^2 + (\Delta + \beta')^2/4}$$

$$E^1_{hA_2g} = \frac{1}{2}\Delta - \frac{1}{2}\beta' + \sqrt{(4/3)\beta^2 + (\Delta + \beta')^2/4}$$

$$E^1_{lA_1u} = \frac{1}{2}\Delta + \frac{1}{2}\beta' - \sqrt{(2/3)\beta^2 + (\Delta - \beta')^2/4}$$

$$E^1_{hA_1u} = \frac{1}{2}\Delta + \frac{1}{2}\beta' + \sqrt{(2/3)\beta^2 + (\Delta - \beta')^2/4}$$

$$E^0_{A_1u} = \Delta \qquad \text{(A4)}$$

where the energy of the ground electronic configuration (Scheme 10) was taken as zero of energy and the subscripts l and h in the left-hand side denote the lowest and the highest level of a given symmetry and spin. The parameter Δ, eq (A3), includes now essential contributions from δ and $U_2 - U_1$ due to the difference between Cr and Fe ions.

JA030027T